Shape and Orientation of Mercury from Radar Ranging Data

J. D. Anderson, R. F. Jurgens, E. L. Lau and M. A. Slade 111

Jet Propulsion Laboratory

California Institute of Technology

Pasadena, California 91109

G. Schubert

Department of Earth and Space Sciences

Institute of Geophysics and Planetary Physics

University of California

Los Angeles, California 90024-1567

Submitted to *Icarus*

19 Pages

3 Figures

1 Table

Key Words: Mercury, Mercury topography, Radar ranging, Crustal thickness

September 22, 1995

Running Head: **Shape and Orientation of Mercury**

Editorial Correspondence and Proofs to:

John D. Anderson

Jet Propulsion Laboratory

Mail stop 30 -230

4800 Oak Grove Drive

Pasadena, California 9 09

(818) 354-3956; john.d.anderson@jpl.nasa.gov; fax (818) 393-0028

ABSTRACT

By means of a topographic Legendre expansion complete through the second degree and order, the systematic error in Mercury radar ranging can be reduced significantly. We interpret the expansion coefficients in terms of a best-fit ellipsoid displaced with respect to the center of mass. The ellipsoid's principal axes are rotated in the equatorial plane such that the long axis is aligned with cartographic longitude 5.3° ± 2.9° (west). The pole location is consistent with the IAU pole, normal to Mercury's orbital plane. There is a significant equatorial ellipticity (a - b)/a = (540 ± 54) × 10^{-6}. The center of figure is offset from the center of mass (C.F. - C.M.) by 640 ± 78 m in the equatorial plane in the direction of cartographic longitude 319.5° ± 6.9°. The magnitude of the center of figure offset implies an excess crustal thickness of 12 km or less, comparable to the Moon's excess. By comparing the equatorial ellipticity with the Mariner 10 gravity coefficient C_{22}, and assuming Airy isostatic compensation, we conclude that Mercury's crustal thickness is in the range of 100 to 250 km.

1 Introduction

Mercury is the least explored of the terrestrial planets. Its known global geophysical properties include i s adius, and gravitational coefficients J_2 and C_{22} (Anderson et al. 1987). n this paper we add to this by using ground-based ada ranging data a d two range determinations from Mariner 10 to determine both the magnitude and direction o the equatorial offset of the center of Mercury's figure from its center of mass. also use these data to find the orientation and major and minor axes of the ellipse which best fits Mercury's equatorial shape. Displacements of the center of figure from the center of ass are known for Earth (Balmino et al. 1973), Moon (Kaula et al. 1972; Bills and Ferrari 1977; Smith et al. 1995), Venus (Bindschadler et al. 1994), and Mars (Standish 1973; Bills and Ferrari 1978). However, there is no estimate in the literature of Mercury's center of figure displacement from its center of mass even though the global equatorial topography of Mercury from ground-based radar ranging has been discussed (Harmon et al. 1986; Harmon and Campbell 1988; Pitjeva 1993). There has also been no determination of the equatorial ellipticity from heretofore published topography or any discussion]) of the geophysical implications of the global equatorial elliptical shape. The shape and orientation of Mercury's equatorial figure and the displacement of this figure from the planet's center of mass place important constraints on the structure of Mercury's interior.

2 Mercury Radar Ranging

A summary and discussion of data used in the fundamental ephemerides DE200/LE200 has been published previously (Standish 1990; Standish et al. 1992). Those data include Mercury radar ranging data spanning the years 1966-1974. We report here on the analysis of the older data plus additional data spanning the years 1974 to 1990. Included are two range fixes from the Mariner 10 Mercury flybys on March 29, 1974 and March 16, 1975 (Anderson et al, 1987). We have excluded the highly noisy 1966 Arecibo data. The current JPL set of reduced Mercury radar ranging data is summarized in Table 1. The Goldstone data are from 34 m and 70 m stations located in California's Mojave desert, the Arecibo data are from Puerto Rico, while the Haystack data are from Tyngsboro, Massachusetts.

The data used for this paper are reduced ranging measurements to Mercury's surface.

Both radar time delay and Doppler data have been used in the reduction (for an explanation of the Doppler-delay technique see e.g. Ingalls and Rainville 1972; Shapiro et al. 1972; Harmon et al. 1986). The 1978-1982 reduced data are from archives at the Harvard Smithsonian Center for Astrophysics (J. Chandler, private communication). All these reduced radar ranging data are suitable for studies of global topography, as reported here, but topographic analysis at higher resolution requires data from an earlier stage in the data reduction (see e.g. Harmon et, al. 1986). The two Mariner range fixes, accurate to ± 1 μs, or about 150 m in distance, are independent of topography, but they help define the absolute location of Mercury's center of mass.

Given the data summarized in Table 1, we have computed ranging residuals referenced to JPL research ephemeris DE242 (E. M. Standish, private communication; Anderson et al, 1995). This ephemeris has been superseded recently by DE403. However the results reported here are insensitive to whether DE242 or DE403 is used as the zero-order model for the linear fit. The important point is that when Mercury ranging residuals are plotted using cartographic longitude, rather than time as independent variable, systematic effects are obvious. These systematic effects have been noted before as a troublesome error source for tests of general relativity, most notably the excess precession of Mercury's perihelion, and models have been introduced for purposes of minimizing the error (Anderson et al. 1991; Pitjeva 1993). We suggest, that the Legendre expansion discussed here is the most effective in removing systematic error introduced by Mercury's topographic variations, at least until new data are available from a Mercury orbiter mission. Such new data could take the form of transponded ranging, similar to the Mariner 9 Mars Orbiter, or perhaps even surface transponded ranging similar to the two Viking Landers. Unfortunately, no Venus orbiter has carried a ranging transponder to date, although work is underway at JPL to use coherent Doppler to improve Venus' ephemeris (Konopliv, private communication). We have removed Venus topography from Venus radar ranging data by using the Pioneer 12 radar altimetry measurements, and one range fix is available from the Galileo spacecraft flyby in 1990 (Anderson et al. 1991). Of all the inner planets, only Mercury currently requires a parameterized topography model for ranging data, analysis.

3 Global Topography

The recommended model for Mercury's radius r, including terms in both latitude and longitude, is a truncated Legendre expansion complete through the second degree and order

$$\begin{aligned} r = R + C_{10}\sqrt{3}\sin\phi + (C_{11}\cos\lambda + S_{11}\sin\lambda)\sqrt{3}\cos\phi \\ + C_{20}\tfrac{\sqrt{5}}{2}(3\sin^2\phi - 1) \\ + (C_{21}\cos\lambda + S_{21}\sin\lambda)\sqrt{15}\sin\phi\cos\phi \\ + (C_{22}\cos 2\lambda + S_{22}\sin 2\lambda)\tfrac{\sqrt{15}}{2}\cos^2\phi \end{aligned} \tag{1}$$

We have augmented the DE242 parameter set, including the mean radius R, by the eight Legendre coefficients in Eq. 1. Then, by linearly correcting DE242's 181 parameters, and by including the eight new parameters, we have repeated the chi-square fit to all the DE242 data, but with 189 rather than 181 degrees of freedom.

The new results for the radius R and the eight Legendre coefficients are

$$R = 2,437,6003\ 2900\ m$$

$$C_{10} = -- 103(1\ i\ 650\ m$$

$$C_{11} = 281 \pm 46\ m$$

$$S_{11} = --240 \pm 43n1$$

$$C_{20} = --2100 \pm 2600\ m \qquad (2)$$

$$C_{21} = --1204.170111$$

$$S_{21} = --100+ 170111$$

$$C_{22} = 293:135\ m$$

$$S_{22} =- 1734:33\ m$$

The errors are taken directly from the covariance matrix. The data weights have been scaled on a data set by data set basis such that the overall standard error for the weighted data is unity (c]li-square = N - 189 = 73346, where N is the number of observations making up DE242). Among the nine topography parameters, there are five significant correlations with absolute magnitude larger than 0.24. The remaining 31 correlations are smaller. The most significant are

$$Corr(R, C_{20}) = 0.9997$$

$$Corr(C_{10}, C_{21}) = -0.3174$$

$$Corr(C_{11}, C_{21}) = -0.5907 \qquad (3)$$

$$Corr(C_{21}, C_{22}) = 0.3040$$

$$Corr(C_{11}, S_{21}) = -0.3719$$

To the first order in the small corrections, we have interpreted the coefficients in terms of a reference ellipsoid. The center of figure is offset from the center of mass (C.F. - C.M.)

by amounts

$$r_c \cos \phi_c \cos \lambda_c = \sqrt{3} C_{11}$$

$$r_c \cos \phi_c \sin \lambda_c = \sqrt{3} S_{11} \qquad (4)$$

$$r_c \sin \phi_c = \sqrt{3} C_{10}$$

The cylindrical coordinates of the position of the center of figure with respect to the center of mass, where ϕ_c is the latitude and λ_c the west longitude are

$$r_c \cos \phi_c = 640 \pm 78\text{m}$$

$$r_c \sin \phi_c = -1780 \pm 1130\text{m}$$

$$\lambda_c = 319.5° \pm 6.9°$$

The latitude ϕ_c is $-70.3° \pm 11.7°$, which implies most of the offset is directed toward the south pole. However, because the radar ranging is restricted to the equatorial region, the polar component of the offset is poorly determined. It will not be known with certainty until data become available from a Mercury orbiter mission.

The orientation of the ellipsoid is defined by three rotation angles. The first rotation is about the polar axis through the cartographic longitude λ_0. The second and third rotations are assumed small such that the longitude λ_P and colatitude θ_P of the ellipsoid's pole are related to small angles u and v by

$$\sin \theta_P \cos \lambda_P = u$$

$$\sin \theta_P \sin \lambda_P = v \qquad (6)$$

The angle λ_0, not necessarily small, is

$$\lambda_0 = \frac{1}{2} \arctan \frac{S_{22}}{C_{22}} = 15.3° \pm 2.9° \qquad (7)$$

The three axes of the ellipsoid arc given by

$$a = R + \frac{\sqrt{15}}{2}\sqrt{C_{22}^2 + S_{22}^2} - \frac{\sqrt{5}}{2}C_{20} = 2,440,623 \pm 108\,\mathrm{m}$$

$$b = R - \frac{\sqrt{15}}{2}\sqrt{C_{22}^2 + S_{22}^2} - \frac{\sqrt{5}}{2}C_{20} = 2,439,305 \pm 113\,\mathrm{m} \tag{8}$$

$$c = R + \sqrt{5}C_{20} = 2,432,900 \pm 8800\,\mathrm{m}$$

The correlation between R and C_{20} significantly reduces the error in the equatorial axes a and b, but the large error in the polar axis c is enhanced. The radar data arc restricted between 12° north and 10° south in latitude, hence geodetic. parameters along the polar axis arc poorly determined. The one-sigma error ellipse associated with the well determined axes a and b is shown in Fig. 1. The two axes arc far from being equal, so wc have definitely determined an ellipticity in the equatorial plane given by $(a - b)/a = (540 \pm 54) \times 10^{-6}$. However, the values for a and b arc consistent with Mercury's reference radius $R_0 = 2,440$ km. This reference radius is an excellent approximation to the mean equatorial radius. The ellipsoid's flattening f, defined by $(\sqrt{ab} - c)/\sqrt{ab}$, is

$$f = -\frac{3\sqrt{5}C_{20}}{2R} = 0.00289 \pm 0.00363 \tag{9}$$

As expected, f is poorly determined and, based on the radar ranging data, consistent with zero.

Radio occultation radii have been determined from Mariner 10's first Mercury flyby in March 1974 (Fjeldbo et al. 1976). At the ingress location the radius is 2439.5 ± 1.0 km at latitude 1.1° and cartographic longitude 292.6°, and at egress the radius is 2439.0 ± 1.0 km at latitude 67.6° and cartographic longitude 101.6° (wc have converted Fjeldbo et al.'s cast longitude to west longitude). The occultation radii are consistent with our results, but they yield little or no information on the best-fit Mercu y ellipsoid because, as pointed out by

Fjeldbo et al., they may be affected by local topography at a level significantly larger than the ± 1.0 km standard error. The occultation heights, referenced to the ellipsoid determined by Eq. 1, are -348 ± 1010 m at ingress and 7110 ± 7450 m at egress, Because of the ellipsoid's relatively small polar axis and the Cl'. - C.M. offset of 1.8 km toward the south pole, the estimated height at the 67.6° latitude location is large but within the! limit of onc standard deviation. Outside of checking for consistency, wc have ignored both occultation radii in our analysis.

Given the principal axes of the ellipsoid, and the angle λ_0, wc next determine the two smal or ient ation angles from

$$
\begin{aligned}
u &= \frac{\text{[illegible]}}{\sqrt{3}C_{20}-\sqrt{C_{22}^2+S_{22}^2}} = 1.73^\circ \pm 3.14^\circ \\
v &= \frac{S_{21}}{\sqrt{3}C_{20}+\sqrt{C_{22}^2+S_{22}^2}} = 1.74^\circ \pm 3.79^\circ
\end{aligned}
\qquad (10)
$$

Because the correlation between u and v is 0.390, wc display the error ellipse in Fig. 2. Note that the pole location determined from radar ranging is consistent with the reference pole, assumed normal to the plane of Mercury's orbit. By computing an inclination angle from the coefficients in Eq. 2, wc have checked that the assumption of small rotations u and v does not bias the pole toward the reference pole. The inclination angle is not significantly different from zero.

4 Geophysical Discussion

The offsets of the center of figure from the center of mass of all the terrestrial planets arc plausibly though not uniquely interpreted as duc to hemispheric asymmetries in crustal thickness. The Moon's offset of the center of figure from the center of mass is about 2 km in a direction away from the Earth and can be explained as duc to a thicker crust on the lunar farside than on the nearside (Kaula et al. 1972; Bills and Ferrari 1977; Smith et al. 1995; Neumann et al. 1995). Mars' 2.5 km offset is in a direction approximately halfway between the Tharsis bulge and the southern highlands and can be understood as duc to thickened crust in these regions (Bills and Ferrari, 1 978; Schubert et al. 1992). The 2.1 km offset of the Earth's figure from its center of mass is in the. direction of the Pacific basin (Lee and Kaula 1967; Balmino et al. 1973) and may be a consequence of the thick continental crust beneath Eurasia compared with the thin oceanic crust beneath the Pacific and]ndian Oceans. Venus' center of figure is displaced from its center of mass by only about 300 m in a direction toward northeastern Thetis Regio near the geometric center of the Aphrodite highland and may be duc to crustal thickening beneath this region (Bindschadler et al. 1994).

Mercury's 640 m equatorial offset of its c.enter of figure from its center of mass is in the direction 319.5° W longitude in the planet's unimaged hemisphere. It is therefore difficult to interpret the planet's center of figure offset fi om its center of mass and relate the direction of this offset to the surface geology, but if we assume that the offset is due to global crustal thickness variations, as is likely for similar offsets on all the other terrestrial planets, then we can usc the offset to constrain the difference between the crustal thicknesses 011 Mercury's unimaged and imaged hemispheres. Mercury's d isplacement of its figu re center from its mass center is only about a third as large as the displacements on Earth, Mars, and the Moon, but it is twice as large as the Venus offset. The Venus center of figure displacement from the center of mass is very small because of the limited areal extent of thickened highland crust on Venus. The relative smallness of the center of figure displacement from the center of mass on Mercury implies that we are not in for any great surprises when wc image the rest of the planet in terms of finding an unusual distribution of basins, highlands and plains compared wi th the imaged hemisphere.

If we usc the formula from Kaula et al. (1 97'2) for the offset of the center of figure from the center of mass (C. F.-C.M. offset), then the hernisphcrically-averaged excess crustal thickness is twice the C. F.-C.M. offset divided by $\Delta\rho/\rho$, where $\Delta\rho$ is the mantle density minus the crusts] density and ρ is the mantle density. For $\Delta\rho/\rho$ equal to 0.1 the excess crustal thickness responsible for the C. F.-C. M. offset is only 12.8 km, The excess crustal thickness could be even smaller if the density of the subcrustal lithosphere on Mercury were larger than the upper mantle density on the Earth or Moon leading to a larger value of $\Delta\rho/\rho$. The excess crusts] thickness responsible for the Moon's C, F.-C.M. offset is about 12 km (Neumann et al. 1995).

The long axis of Mercury's equatorial elliptical shape is oriented toward 15° W longitude in qualitative agreement with the locations of the two main equatorial highlands described by Harmon et al. (1986) and Harmon and Campbell (1988). The measured equatorial ellipticity of Mercury, 540 x 10^{-6}, corresponds to a value of C_{22} equal to 5.4 x 10-5 on the assumption that Mercury is a constant density tri-axial ellipsoid (the formula for C_{22} of an ellipsoid of constant density with principal axes a,b,c (a>b>c) is approximately $(a^2 - b^2)/20a^2$ (Yoder, 1 995)). The value of C_{22} inferred from the Mariner 10 flybys is 1.0 ± 0.5 x 10^{-5} (Anderson et al. 1987). The large value of C_{22} associated with the equatorial ellipticity compared with the measured value of C_{22} implies that Mercury's equatorial ellipticity is isostatically compensated. If wc assume that the compensation is due to Air-y isostasy associated with a variable thickness crust, then it can be shown that the mean crustal thickness or compensation depth H is given approximately by

$$\frac{H}{a} = \frac{1}{4} C_{22}(\text{observed}) \left[\frac{(a-b)}{10a} \frac{\rho_c}{\bar{\rho}} \right]^{-1} \tag{11}$$

where ρ_c is the crustal density and $\bar{\rho}$ is the mean density of Mercury. The expression in Eq. 11 is derived by using the formula for B-A (B and A are the equatorial moments of inertia, B>A) of a constant density tri-axial ellipsoid and applying this formula to the surface ellipsoid with density ρ_c and the compensation ellipsoid of density $(\rho_m - \rho_c)$ (ρ_m is the subcrustal density) (Fig. 3). The compensation ellipsoid has its long equatorial axis at 90° to that of the surface ellipsoid (Fig. 3) and the difference in its equatorial radii is given by $(a - b)(\rho_c/(\rho_m - \rho_c))$. For the values of C_{22}(observed) and (a-b)/a given above and for $\rho_c/\bar{\rho}$ equal to 3/5.4, Eq. 11 gives $H/a = 1/12$ or $H = 203$ km. Since the error in the determination of C_{22} is 0.5×10^{-5}, H could be a factor of 2 smaller or a factor of 1.5 larger.

For the Moon, C_{22} is about 2.2×10^{-5} (Lemoine et al. 1995). If we use 2.4 km for the difference in the Moon's equatorial radii (Kaula et al. 1973; Zuber, private communication) and $\rho_c/\bar{\rho}$ equal to 2.9/3.3, then according to Eq. 11 the lunar mean crustal thickness or depth of compensation H is about 72 km. The mean crustal thickness of the Moon is about 61 km (Neumann et al. 1995). Comparison of the observed C_{22} of the Moon with its equatorial ellipticity based on Apollo 16 and Clementine data gives a reasonable estimate of the Moon's mean crustal thickness. The same may be true for Mercury, although the uncertainty in Mercury's C_{22} is large enough that the inferred mean crustal thickness for Mercury can range between about 100 and 250 km.

1 -

5 Acknowledgements

We acknowledge discussions with E. M. Standish, Jr. regarding the data analysis and the J]'], ephemeris system. We thank him for giving us unlimited access to his computer files. A. J. Anderson encouraged us to pursue the geophysical aspects of the data analysis. We thank W. B. Moore for helpful discussions and for his assistance in the preparation of Fig. 3. The research described in this paper was carried out by the Jet l'repulsion Laboratory, California Institute of Technology, and was sponsored by the Ultraviolet, Visible, and Gravitational Astrophysics Research and Anal ysis Program through an agreement with the National Aeronautics and Space Administration. Support from NASA NSG 7315 for G. S. is also acknowledged.

6 References

Anderson, J. D., G. Colombo, 1'.11. Esposito, E. L. Lau, and G. B. Trager 1987. The mass, gravity field, and ephemeris of Mercury. *Icarus* 71, 337-349.

Anderson, J. D., M. A. Slade, R. F. Jurgens, E. L. Lau, X X Newhall, and E. M. Standish Jr. 1991. Radar and spacecraft ranging to Mercury between 1966 and 1988. *Proc. Astron. Sot. Australia* **9**, *324.*

Anderson, J. D., E. 1,. Lau, T. P. Krisher, D. A. Dicus, D. C. Rosenbaum, and V. 1,. Teplitz 1995. Improved bounds on non-luminous matter in solar orbit. *Astrophys. J.* 448, 885-892.

Balmino, G., K. Lambeck, and W. M. Kaula 1973. A spherical harmonic analysis of the Earth's topography. *J. Geophys. Res.* 78, 478-481.

Bills, B. G., and A. J. Ferrari 1977. A harmonic analysis of lunar topography. *Icarus* 31, 244-259.

Hills, B. G., and A. J. Ferrari 1978. Mars topography harmonics and geophysical implications. *J. Geophys. Res.* 83, 3497-3508.

Bindschadler, D. 1,., G. Schubert, and 1'. G. Ford 1994. Venus' center of figure - center of mass offset. *Icarus* 111 , 417 -432.

Fjeldbo, G., A. Kliore, D. Sweetnam, P. Esposito, B. Seidel, and 'J'. Howard 1976. The occultation of Mariner 10 by Mercury. *Icarus* **29, 439-444.**

Harmon, J. K., 1). B. Campbell, D. L. Bindschadler, J. W. Head, and 1. 1. Shapiro 1986. Radar altimetry of Mercury: A preliminary analysis *J. Geophys. Res.* 9 1 , 385-401.

Harmon, J. K, and 1). B. Campbell 1988. Radar observations of Mercury. in *Mercury* (F. Vilas, C. R. Chapman, and M. S. Matthews, Eds.), pp. 1 01-117. Univ. of Arizona Press, Tucson.

Ingalls, R. P., and 1,.1'. Rainville 1972. Radar measurements of Mercury: Topography and scattering characteristics at 3.8 cm. *Astron. J.* 77, 185-190.

Kaula, W. M., G. Schubert, R. E. Lingenfelter, W. L. Sjogren, and W. R. Wollenhaupt 1972. Anal ysis and interpretation of lunar laser altimetry. *Proc. 7'bird Lunar Planet.*

Sci. Conf., 2189- '2204.

Kaula, W. M., G. Schubert, R. E. Lingenfelter, W. L. Sjogren, and W. R. Wollenhaupt 1973. Lunar topography from Apollo 15 and 16 laser altimetry. *Proc. Fourth Lunar Sci. Conf., Geochimica et Cosmochimica Acts, Suppl.* **4, Vol.** 3, 2811-2819.

Lee, W. 11. K., and W. M. Kaula 1967. A spherical harmonic. analysis of the Earth's topography. *J. Geophys. Res.* **72**, 753-758.

Lemoine, F. G., D. E. Smith, M. T. Zuber, G. A. Neumann, and D. D. Rowlands 1995. GLGM-2: A 70th degree and order lunar gravity model from Clementine and historical data. Preprint.

Neumann, G. A., M. T. Zuber, D. E. Smith, and F. G. Lemoine 1995. The lunar crust: Global structure and signature of major basins. *Preprint.*

Pitjeva, E. V. 1993. Experimental testing of relativistic effects, variability of the gravitational constant, and topography of Mercury surface from radar observations 1964-1989. *Celes. Mech. Dynam. Astron.* **55, 313-321.**

Schubert, G., S. C. Solomon, D. L. Turcotte, M. J. Drake, and N. H. Sleep 1992. Origin and thermal evolution of Mars. In *Mars* (H. H. Kieffer, B. M. Jakosky, C. W. Snyder, and M. S. Matthews, Eds.), pp. 147- 183. Univ. of Arizona Press, Tucson.

Shapiro, I. I., S. H. Zisk, A. E. E. Rogers, M. A. Slade, and T. W. Thompson 1972. Lunar topography: Global determination by radar. *Science* **178, 939-948.**

Smith, D. E., M. T. Zuber, G. A. Neumann, and F. G. Lemoine 1995. The topography of the Moon from Clementine LIDAR. Submitted to *J. Geophys. Res.*

Standish, E. M. 1973. The figure of Mars and its effect on radar ranging. *Astron. Astrophys.* **26, 463-466.**

Standish, E. M. 1990. The observational basis for JPL's DE200, the planetary ephemerides of the Astronomical Almanac. *Astron. Astrophys.* **233, 252-271.**

Standish, E. M., X X Newhall, J. G. Williams, and D. K. Yeomans 1992. Orbital ephemerides of the Sun, Moon, and planets. In *Explanatory Supplement to the Astronomical Almanac* (P. K. Seidelmann, Ed.), pp. 279323. Univ. Sci. Books, Mill Valley.

Yoder, C. F. 1995. Astrometric and geodetic properties of Earth and the solar system. In *Global Earth Physics, A handbook of Physical Constants* (T. J. Ahrens, Ed.), pp. 1 - 31. Amer. Geophys. Union, Washington.

7 Figure Captions

FIG. 1. one-sigma error ellipse for the ellipsoid's principal axes a and b. The best-fit deviations from the reference radius R_0 as determined by radar ranging data are indicated by the solid square in the center of the error ellipse. The dashed line represents values of a and b for which their mean is equal to the reference radius R_0 = 2440 km.

FIG. 2. One-sigma error ellipse for the small polar angles u and v. The IAU reference pole normal to Mercury's orbital plane is at the origin of the dashed axes. The location of the ellipsoid's pole as determined by radar ranging data is indicated by cartographic longitude λ_P and colatitude θ_P.

FIG. 3. Sketch of the mass excesses and deficits associated with the equatorial ellipticity of a planet, and its Airy compensation ellipse. The long axes of the surface and compensation ellipses are at right angles. H is the compensation depth or mean crustal thickness. ρ_c is the crustal density and ρ_m is the subcrustal density.

8 Tables

TABLE I

Mercury **Radar-Ranging Measurements**

Timespan	Antenna	Number of Observations
1967-1971	Arecibo	85
]966-1971	Haystack	217
1971-1974	Goldstone	38
1974-1975	Mariner 10	2
1978-1982	Arecibo	157
1986-1990	Goldstone	13'2

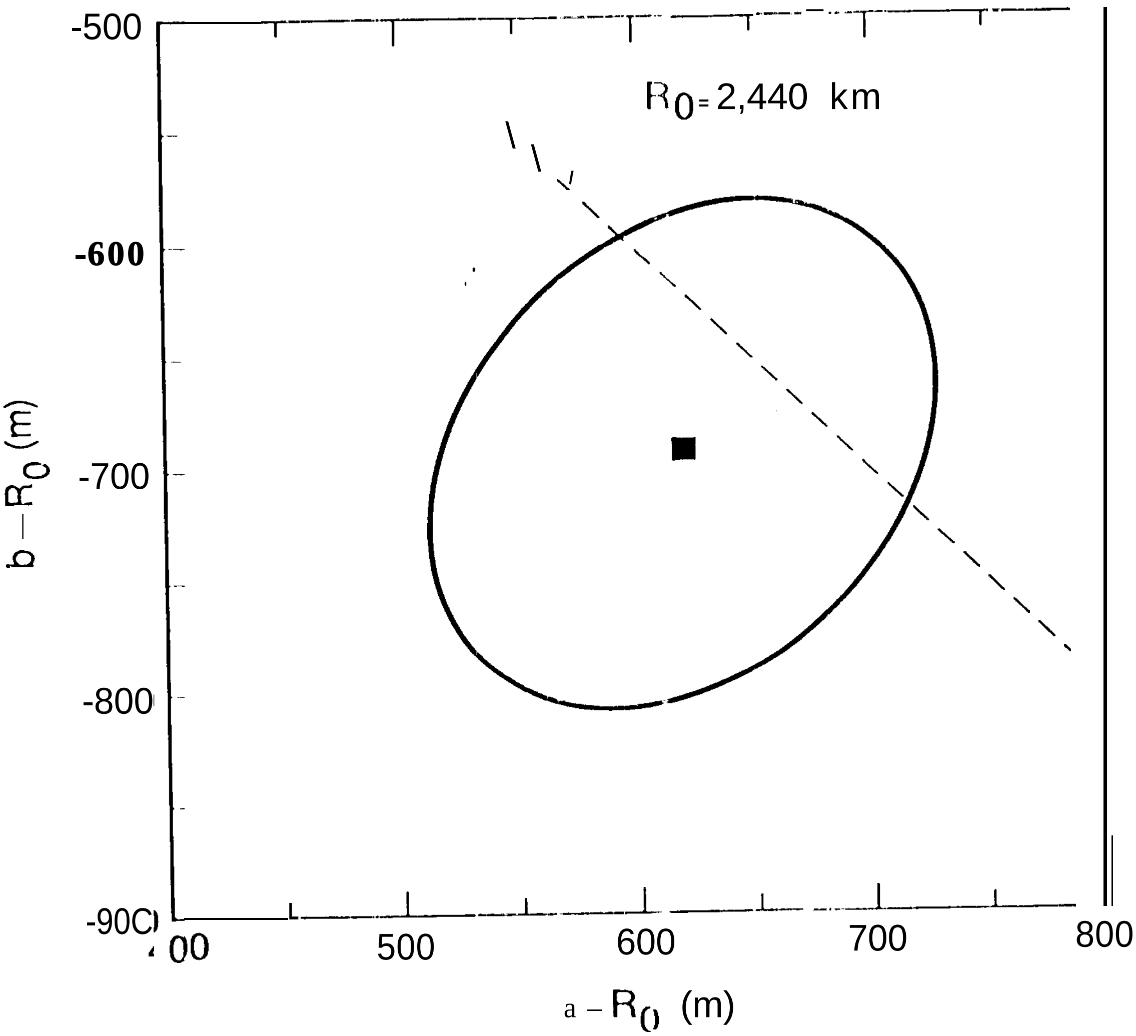

R0 = 2,440 km
-500
-600
-700
-800
-900
400
500
600
700
800
b − R0 (m)
a − R0 (m)

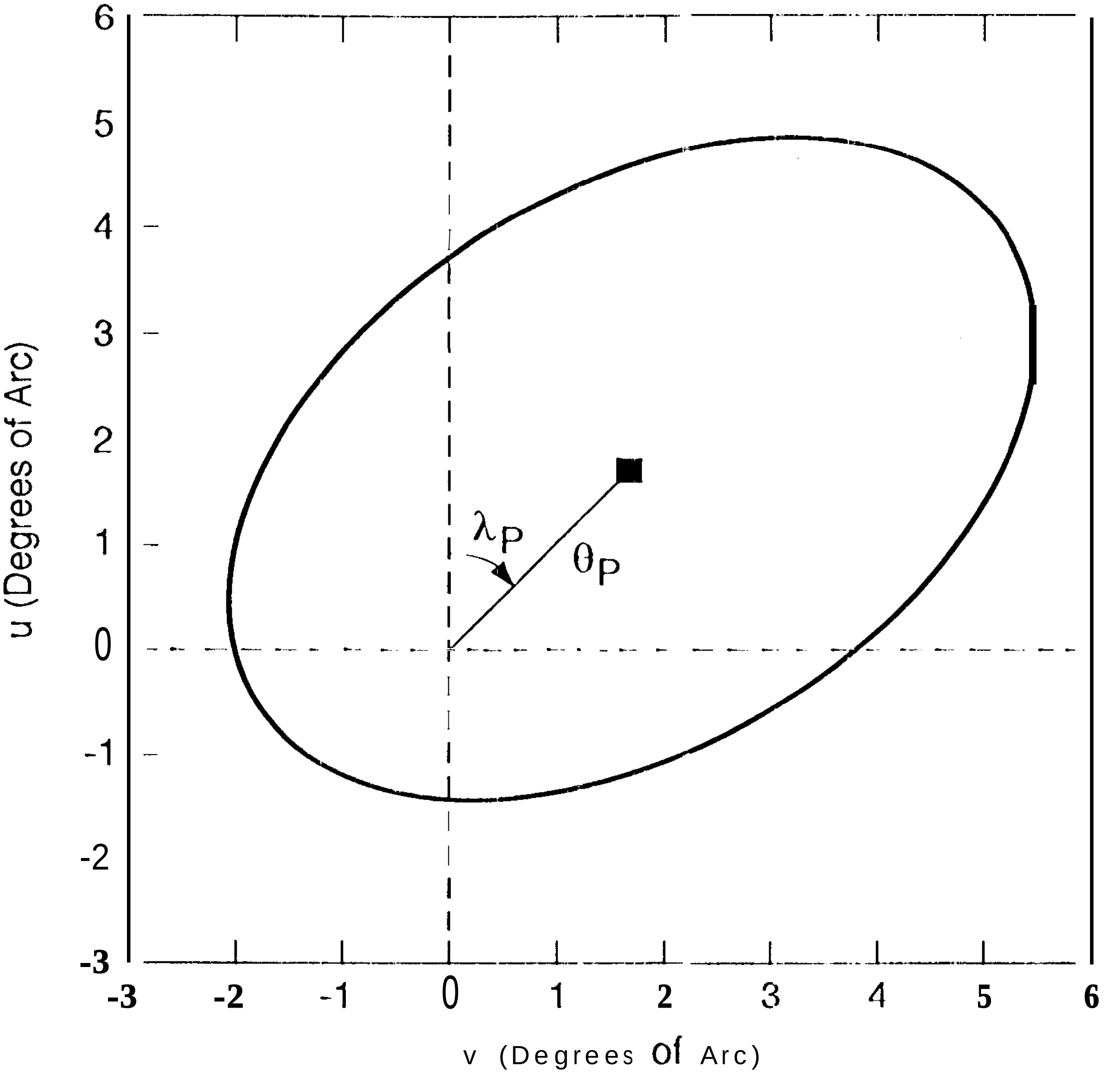

6
5
4
3
2
1
0
-1
-2
-3
u (Degrees of Arc)
-3
-2
-1
0
1
2
3
4
5
6
v (Degrees of Arc)
λ_P
θ_P

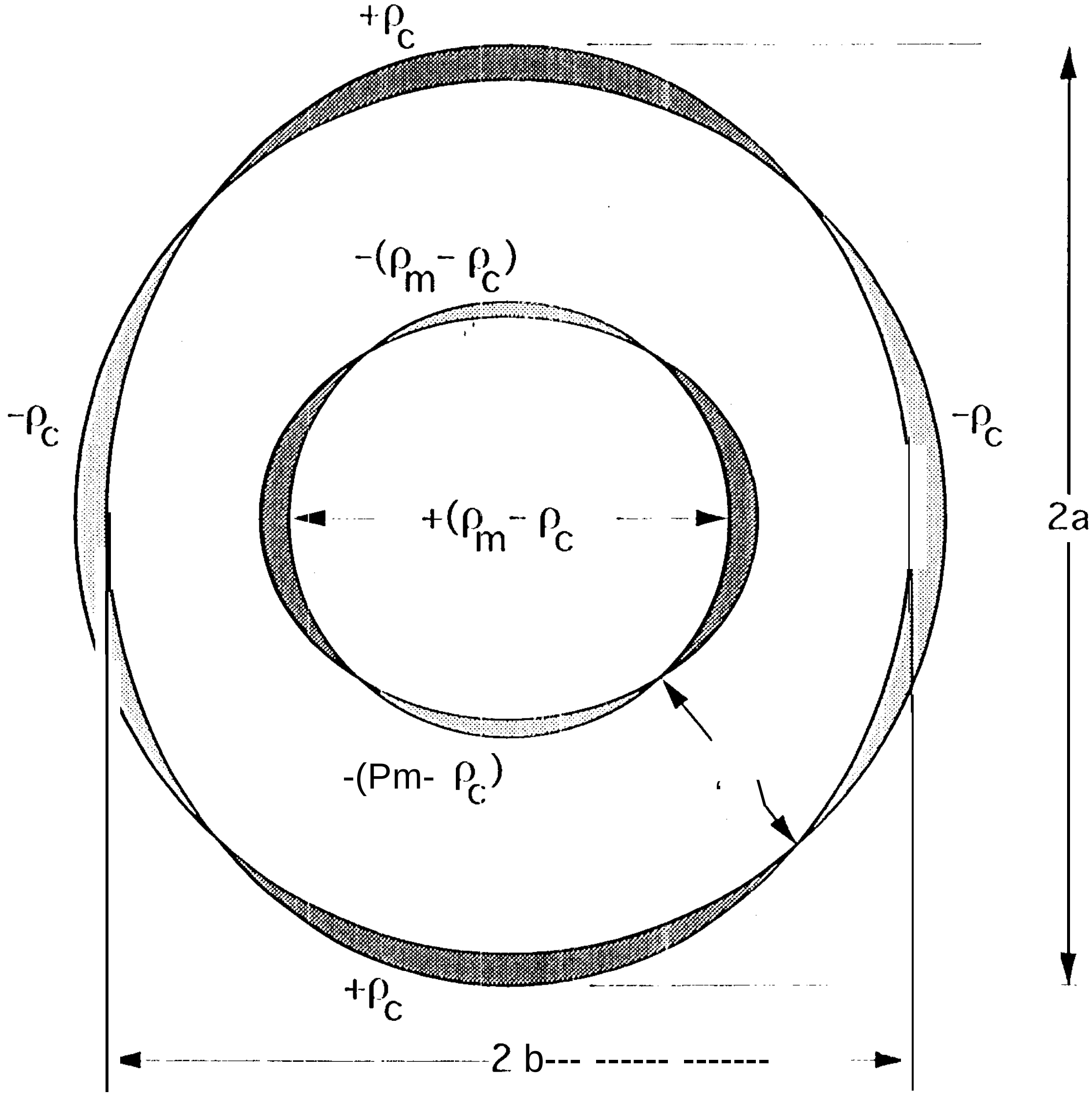
+ρc
-(ρm- ρc)
-ρc
-ρc
+(ρm- ρc
2a
-(Pm- ρc)
+ρc
2 b